The Song Dynasty Shipwreck Monitoring and Analysis Using Acoustic Emission Technique

Qi Zhao [1], Dong Zhao [1,*], Jian Zhao [1] **and Lihua Fei [2]**

[1]   School of Technology, Beijing Forestry University, Beijing 100083, China
[2]   Quanzhou Maritime Museum Fujian, Fujian 362000, China
*   Correspondence: zhaodong68@bjfu.edu.cn

Abstract: The monitoring of acoustic emission (AE) has allowed tracing of the damage in wooden cultural objects exposed to variations in ambient relative humidity (RH). A year-long on-site AE monitoring of the Song Dynasty shipwreck confirmed the usefulness of the technique in tracing climate-induced damage in wood. New coupling material is tested to make it conform to the conservation rules which is non-corrosive to monitoring objects and a reversible operation. As sensitive parameter of wood damage caused by variations RH, the accumulated ringing counting tends to increase with the increase of daily fluctuation of RH (DFRH). In addition, the damage of wooden cultural objects during shrinkage is stronger than that during swelling. The relationship between the probability of AE activity and the daily DFRH is established and it is determined that the daily variation of RH for long-term protection of the Song Dynasty shipwreck should be controlled within 4%, and an early warning will be given if it exceeds 10%.

Keywords: non-destructive; acoustic emission technique (AET); large marine wooden relic; environmental relative humidity (RH); the daily fluctuation of RH (DFRH)

1. Introduction

The Song Dynasty shipwreck in Quanzhou Bay (AD 960-1279) is one of the most important archaeological discoveries in China [1]. In spite of the fact that the technicians adopt various effective protective measures by using physical and chemical techniques under the limited condition, the Song Dynasty shipwreck remained, basically, intact for nearly 40 years. However, exhibited in an open display environment for many years, the deterioration trend for shipwreck wood intensifies and the long-term stable preservation of a shipwreck has difficulties. Cracks, deformation, and other physical damage (Figure 1) caused by stress-induced by changes in relative humidity (RH) and moisture content [2].
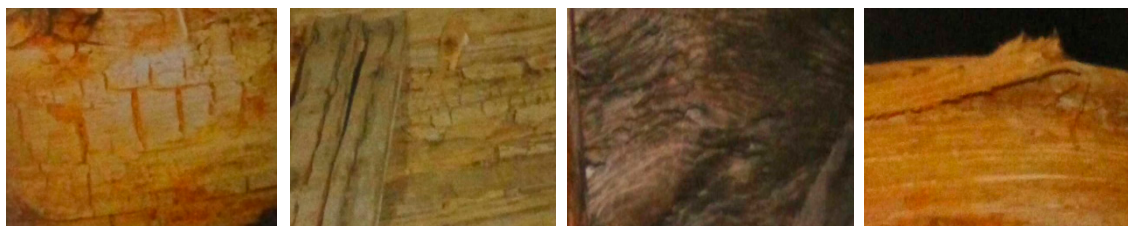
Figure 1. Physical damage from left to right: Lateral crack, fracture, distortion, warpage.

From the degree and scope of damage to shipwreck wood, cracking, deformation, and other physical damage caused by moisture content and RH are common. The change of moisture content

will result in the uneven distribution of moisture on the surface and inside of the material, which has a great influence on the structure of wood. Wood is an anisotropic material that is organized in a complex hierarchical structure [3]. With the change of RH, the rapid loss of moisture during drying will result in uneven distribution of stress on the surface and inside of wooden object. The compressive stress on the internal unit area is small, while the tensile stress on the surface area is large, which leads to the cracking of the wood surface. It is necessary to protect The Song Dynasty shipwreck kept in the Quanzhou museum where the RH is controlled.

More and more researchers applied advanced technologies to protect wooden historical objects, so that technologies can offer help to the protection of cultural heritage. Mizuno et al. [4] firstly applied synchrotron X-ray microtomography to wood identification of an old wooden mask. After that, Stelzner and Million [5] also used X-ray Computed Tomography to scan the archaeological wood and reconstruct the CT images, which were used to analyze the annual growth rings and species of archaeological wood. In order to identify carbon-based pigments in four colorful wooden sculptures of the Jesuit Mission La Trinidad, Tomasini et al. [6] utilized Raman spectroscopy to distinguish these pigments. Park et al. [7] successfully identified the types of trees and surface materials of a lacquered wooden coffin by using Pyrolysis/gas chromatography/mass spectrometry. In the same year, Howe et al. [8] helped archaeologists analyze the pigments of a sub-set of polychromed wooden Andean ritual drinking cups called qeros and its chronological marker by means of X-ray diffraction, X-ray fluorescence spectroscopy, and Raman spectroscopy.

Colombini et al. [9] analyzed chemical characterizations of archaeological lignin of ancient ships of San Rossore (Pisa, Italy) by using Py GC/MS, NMR spectroscopy and GPC analysis technology. Sandak et al. [10] applied Fourier transform near infrared (FT-NIR) spectroscopy to measure cellulose, lignin, crystallinity, and the degree of polymerization for help experts to evaluate the degradation state of the oak pieces of the archaeological wood. Lobb et al. [11] successfully measured and modeled archaeological wood by means of a 3D laser scanner. Nowak et al. [12] utilized the Resistance drilling method to assess the degradation state of wooden buildings of historical value. Tamburini et al. [13,14] used Py-GC/MS to analyze the degradation state of samples of ca. 3000 years old oak wood from the Biskupin site, and then combined attenuated total reflectance Fourier transform infrared spectroscopy (ATR-FTIR) and analytical pyrolysis to evaluate the degradation state of wood samples from dry archaeological sites in Egypt [15]. Raposo et al. [16] utilized resistograph to determine the dimension of the degradation and degraded zones of wood structures.

The researchers mentioned above solved the problem of the archeological wood components and the degradation state of archeological wood. There are also some specialists who focus on evaluating consolidation effectiveness of polymeric product and defect detection. Bardet et al. [17] used high-resolution solid-state NMR to analyze polymeric products added to archaeological wood. Chiantore et al. [18] studied the wood finishes of artworks by using Mid-IR fiber-optic reflectance spectroscopy (FORS). It can quickly and reliably detect the wood finishes. Henriques and Neves [19] used SDT methods of drill resistance and penetration resistance to evaluate consolidation efficiency of scots pine wood consolidated by a polymeric product.

Sfarra et al. [20] applied Holographic Interferometry (HI), Infrared Vision, and X-Ray Fluorescence (XRF) spectroscopy to analyze defect sizes of a statue named "Virgin with her Child" (14th century). Re et al. [21] built a facility based on an X-ray source, a linear X-ray detector, and a high precision mechanical system. It is used to detect a masterpiece of a writing cabinet more than 3 m high called "doppio corpo". Bulcke et al. [22] applied tX-ray CT scanning to wooden musical instruments. Perez et al. [23] used a vibration-based NDT method to assess the damages and structural modification of wooden musical instruments. Fang et al. [24] analyzed the damage of cultural wooden objects by means of air-coupled ultrasonic (ACU).

The researchers mentioned above made use of advanced technologies to provide technical support for evaluating the damage and reinforcement effect. For wooden cultural relics, the relative humidity changes at any time which lead to shrinkage and swelling of cultural wooden objects.

Therefore, Senni et al. [25] took advantage of a mobile device based on a NMR single-sided sensor to track the moisture content of a poplar wood panel. Konopka et al. [26] monitored a clavichord's three-dimensional deformations caused by RH by means of photogrammetric methods. However, this method can only measure the deformation. The internal damage cannot be obtained in time.

Archaeological wood, as a natural material, decomposes slowly due to various biological factors. However, for the protection of wooden artifacts, in addition to knowing its current state (degradation, structure, etc.), long-term and real-time monitoring should also be carried out, which plays an important role in the long-term preservation of wooden artifacts significance. The Song Dynasty shipwreck can be considered a large sized wooden cultural relic. In order to be able to determine the suitable range of RH for long-term preservation of the shipwreck, real-time monitoring is necessary. This paper chose acoustic emission technology based on the understanding of various technologies.

Acoustic emission (AE) monitoring is an important non-destructive tool to track the evolution of damages in material and has also been used in wood science [27–30]. Many researches dealt with the relationship between the stress level in wood under flexural loading and AE due to the fracture process [31–33]. In addition, the effects of external parameters have been also reported [34,35], especially the variation in RH and temperature [36]. Analyzing the acoustic energy level has led to differentiating micro-fractures (low energy) from surface shrinking during drying [37]. Lamy et al. [38] studied the failure process of Douglas fir under monotonic loading by using acoustic emission measurements, digital image acquisition, and force-displacement curve analysis. The results show that crack initiation and crack propagation detected by AE activities is in line with the image analysis results. Moreover, some of these authors [37,39] applied acoustic emission technology (AET) to study the effects of crack initiation and growth of wood materials in the drying process. Rescalvo et al. [40] investigated the application of acoustic emission using multi-resonant sensors and considered that this method has a good application prospect for health monitoring of retrofitted wood elements in the real world. In addition, Reiterer et al. [33] used AET to investigate the fracture properties of softwood and hardwood materials under open mode loading and proposed combining AET with microscopic observations of fracture surfaces to study the shearing fracture behavior of ageing wood. Diakhate et al. [41] applied AET to analyze the fracture in wood material of Double Cantilever Beam specimens under open mode loading.

However, in spite of its wide use in various fields, AE has been used very little to monitor wooden cultural heritage objects. In order to understand the deformation and fracture characteristics of old wood, Ando et al. [42] studied the process of microscopic shearing fracture by AE features and observing the fracture surface under a scanning electron microscope (SEM). These results indicated that at low load levels, the incidence of AE from old wood was greater than in new wood. In addition, the period over which AE with small amplitudes were frequently generated was longer in the old wood than in new wood. Jakiela et al. [43,44] indicated that AE can track the evolution of damage at the microlevel, which preceded failure of wood discernible from the macroscopic perspective. The energy of acoustic emission is correlated to the temperature change. Conte et al. [45] applied AE Technology to detect the xylophagous insects and more specifically oligomerus and relative species in wooden cultural heritage musical instruments kept in European museums and proved that AE can track insect activity.

Above all, as a non-destructive testing method, acoustic emission has high sensitivity, on-line monitoring, etc., and it is especially suitable for long-term monitoring of large wooden cultural objects. Acoustic emission is a phenomenon in which a material or structure is deformed or broken by an internal force or an external force to release strain energy in the form of an elastic wave. The acoustic emission elastic wave can reflect some physical properties and damage of the material. Therefore, it can judge a certain state of the material or structure by detecting the acoustic emission signal. Compared with other non-destructive testing methods, acoustic emission technology has the following characteristics:

- Ability to monitor samples dynamically and in real-time;

- Large monitoring area and high efficiency, especially suitable for monitoring large structures;
- Wide range of applications. Acoustic emission technology is suitable for almost all materials and is not affected by size, working environment, and other factors of the object being tested;
- Acoustic emission technology is a passive detection. Acoustic emission signal energy comes from the object being detected. Therefore, the information carried by the signal directly reflects the state of the detected object.

Hence, this paper presents and illustrates the method for the non-destructive investigation of wooden objects with cultural heritage relevance and applies this method to study the characteristics of marine archaeological wood. In the following section, the first subsection is fully devoted to the choice of a coupling material. The Song Dynasty shipwreck is monitored using AE after giving a device to fix the acoustic emission sensor to a large marine wooden relic. An acoustic emission signal means a damage. It is not until the RH is converted into the daily fluctuation of RH (DFRH) and compared with acoustic emission parameters that a certain acoustic emission parameter sensitive to the shipwreck damage mechanism can be discovered. Finally, the relationship between the probability of AE activity and the daily DFRH is established. The aims of this research step were to evaluate the impact of an ambient relative humidity (RH) potential impact of an ancient wooden shipwreck non-recoverable damage evolution in order to provide suggestions for regulating its use and improving its conservation.

2. Materials and Methods

2.1. Sample Descriptions

An about 800 years old Chinese fir plate with a width of 200 mm and a thickness of 50 mm was chosen for this paper. As shown in Figure 2, four sensors are placed on the Chinese fir plate to monitor Chinese fir plate exposed to RH. The distance between sensors in longitudinal direction is 200 mm and cross grain direction is 100 mm.
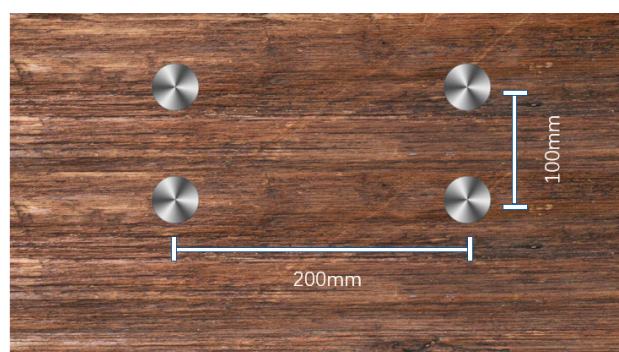
Figure 2. Sensors installation location diagram.

2.2. Experimental Set-up

2.2.1. Coupling Material

Generally, there should be a layer of couplant between the acoustic emission sensor and the object to be detected in order to reduce the influence of air on the detection effect. Currently, the coupling is achieved by means of an adhesive bonding or grease couplant, such as 7501 high-vacuum silicone grease. However, using an adhesive bonding or grease couplant was unacceptable, as they would have contaminated the surface of wood when the technique was finally applied to monitoring authentic works of cultural heritage. Therefore, it becomes the primary problem to choose which couplant can be used.

After determining the working principle and function of the couplant, the material that can be used as couplant is selected. The principles of selection are as follows:

- Non-corrosive monitoring objects;
- Have a certain degree of elasticity;
- The performance is close to the standard couplant.

According to the above principles, four materials that can be used as couplant are found, namely wheat flour, ethylene-vinyl acetate copolymer (EVA), calcium carbonate, and aluminosilicate (Figure 3).

Figure 3. From left to right: Wheat flour, ethylene-vinyl acetate copolymer (EVA), calcium carbonate, aluminosilicate.

In the same specimen and the same position, the lead breaking was used to compare the four materials with air and 7501 high-vacuum silicone grease.

In AE monitoring technology, the AE signal is transformed from the feature extraction circuit into several signal characteristic parameters, such as amplitude, energy, ringing counting, and so on. The mechanical damage of wood is mainly caused by burst signals that have two important parameters, amplitude and energy. Therefore, the focus of this study is to compare the differences in amplitude and energy between different materials (Figure 4).
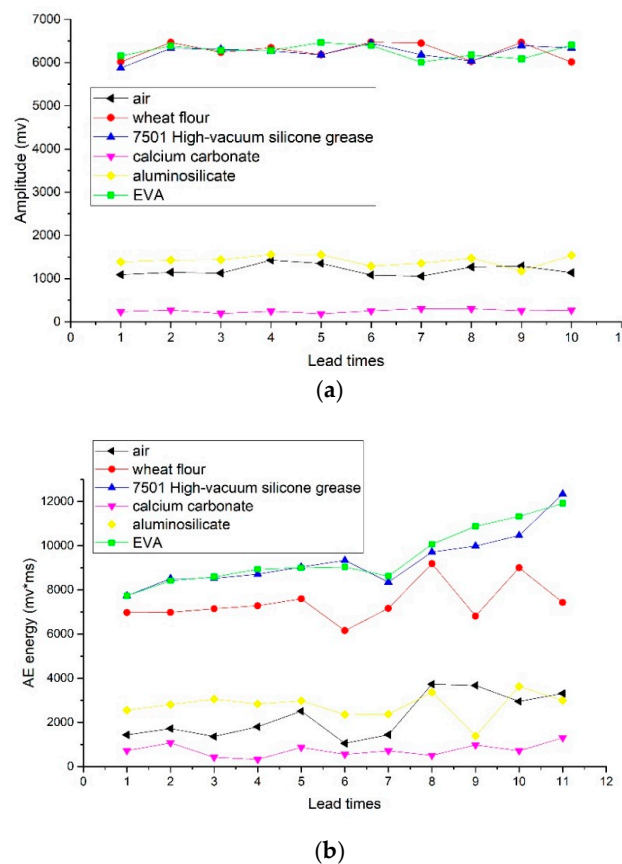
Figure 4. Amplitude and energy of acoustic emission signals with six different materials as couplant.

Figure 4 illustrates the amplitude of the six materials acting as the couplant, analyzed by the lead-breaking test. As can be seen in the graph, the six materials are divided into two types roughly. The first type includes aluminosilicate, calcium carbonate, and air. Amplitude response of lead break signal is similar for these three materials which is too different from the standard couplant to conform to the principle, so it is not accepted. The second type is standard couplant, wheat flour and EVA. As shown in Figure 4a, there is little difference in amplitude response of lead break signal among the three. According to Figure 4b, the difference in energy response between wheat flour and standard couplant is bigger than between EVA and standard couplant. Furthermore, wheat flour will deteriorate during long-term use. Nevertheless, the difference of amplitude response and energy response between EVA and the standard couplant is minimal, and they will not have contaminated the authentic works of cultural heritage. As a result, this paper chooses EVA as a special couplant for ancient wooden ships.

2.2.2. Monitoring Location and Parameter Setting

Acoustic emission detection system of the Song Dynasty shipwreck in the Quanzhou bay monitors one location that is on the partition (Figure 5). The partition materials are chiefly Chinese fir that have no obvious damage. Since the wooden ship is placed in a public environment, we did a test about whether visitors would affect the signal collection before the formal monitoring of the shipwreck. The results show that visitors will increase the background noise in the signal collection process, which does not affect the collection of acoustic emission signals. Therefore, the influence of visitors on the signal can be ignored.
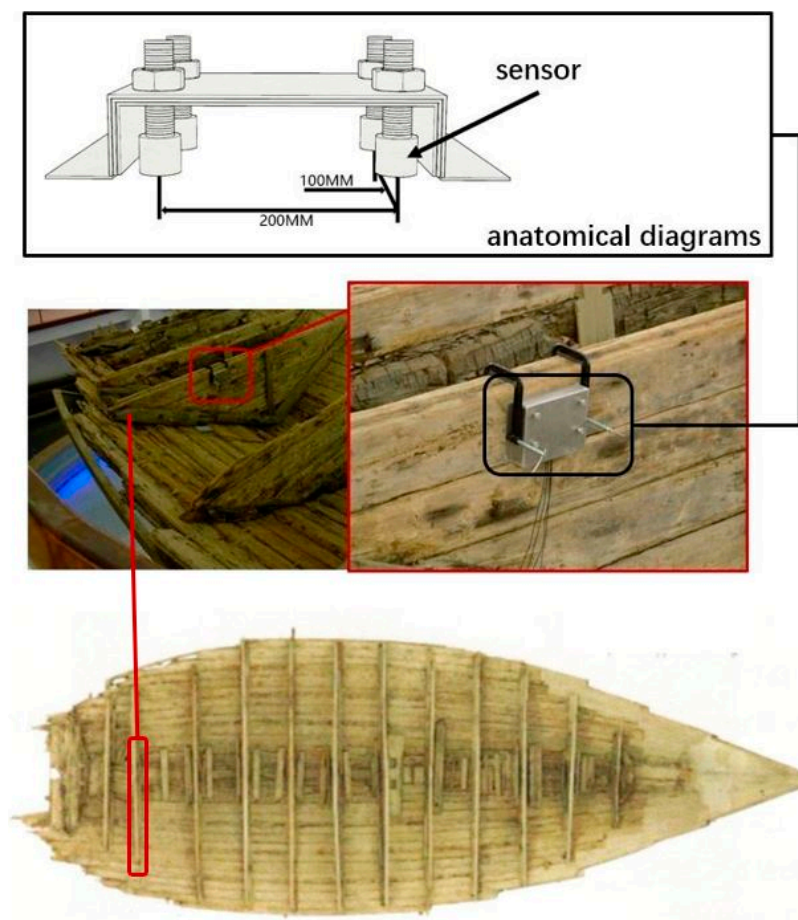
Figure 5. The shipwreck and four acoustic emission sensors coupled to the partition during on-site monitoring of the wooden object.

In order to solve the problem of sensors fixing and reducing the interference of environmental noise, a sound insulation cabin is designed with multiple structures (Figure 6). The inner side is made of two layers of sound insulation materials, which can protect AE sensors from environmental noise. At the same time, AE sensors are fixed in the sound insulation cabin physically, which can avoid re-damage to the tested object, especially for cultural heritage objects.
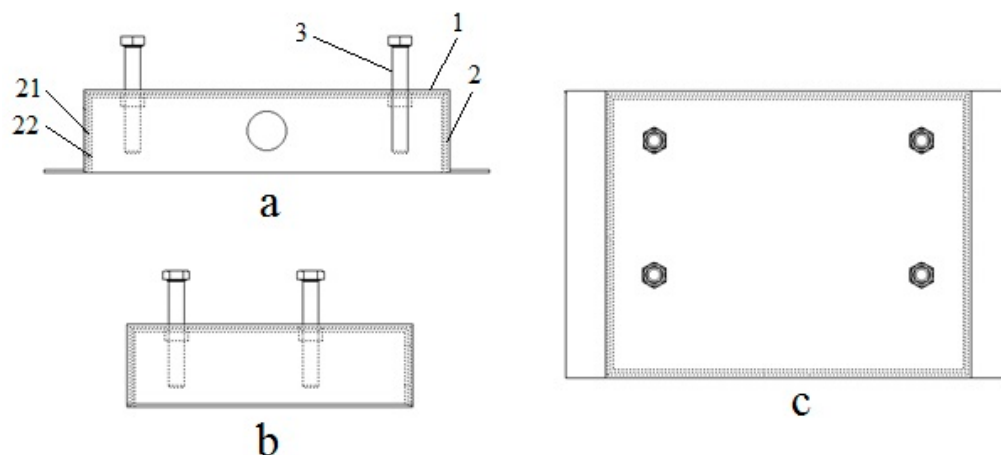
Figure 6. Schematic diagram of a three-dimensional structure of a sound insulation cabin: Front view (**a**), side view (**b**) and top view (**c**), where 21 and 22 represent a sound insulation and 3 is used to fix the acoustic emission (AE) sensors.

At the same time, the spacing of the sensor is set as follows: A distance of 200 mm along the direction parallel to the fibers and up to 100 mm in the direction perpendicular to the fibers [44].

An acoustic emission signal analyzer 8-channel system (from Beijing Softland Times Scientific & Technology Co. Ltd., China) was used to gather the AE signals (see Figure 7). The AE signals were measured with a SR-150 piezoelectric sensor in the [50–400 kHz] frequency range. The acoustic signals were amplified with a gain of 90 dB. The acoustic signals were acquired with a sampling rate of 3 MHz by means of Acoustic Emission Analyzer. A total of 45 mv was selected as the threshold voltage to trigger permanent storage of the AE signals [42].
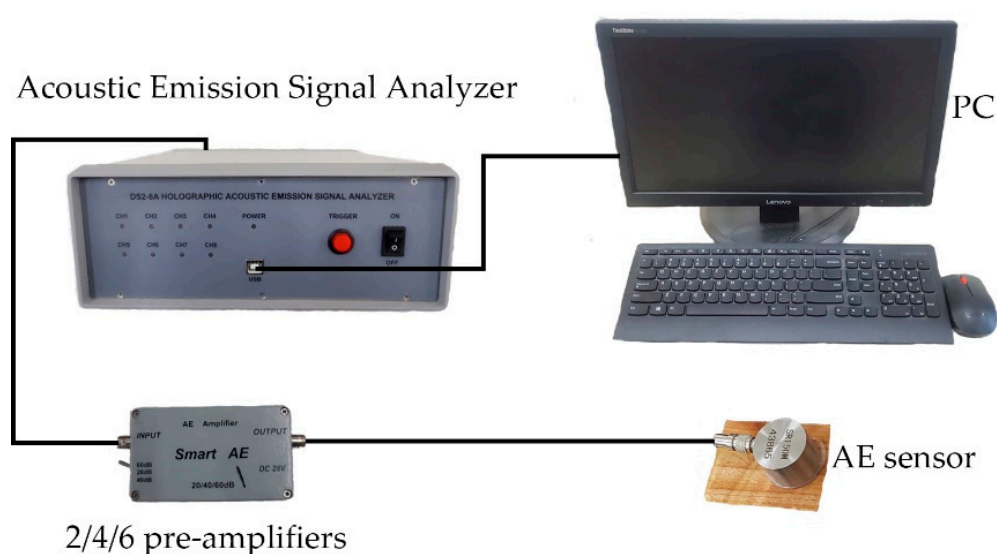
Figure 7. A diagram to show the instrument connection for acoustic emission.

3. Results and Discussion

3.1. Determination of Acoustic Emission Characteristic Parameters

Environmental relative humidity (RH) variation is almost the same in the Quanzhou Bay Exhibition Hall of the Song Dynasty shipwreck every year. Therefore, this study roughly assumed the environmental relative humidity (RH) changes in a cycle of one year (Figure 8).
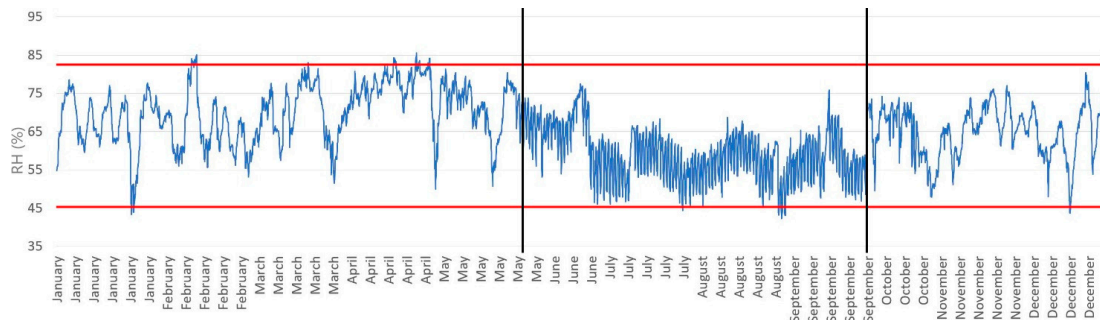
Figure 8. Environmental relative humidity variation in the Quanzhou Bay Exhibition Hall of Song Dynasty shipwreck.

After monitoring throughout the year, AE tracing system collected a total of 73 AE events. The time domain diagram of two typical signals is shown in Figure 9.

(**a**)　　　　　　　　　　　　　　　(**b**)
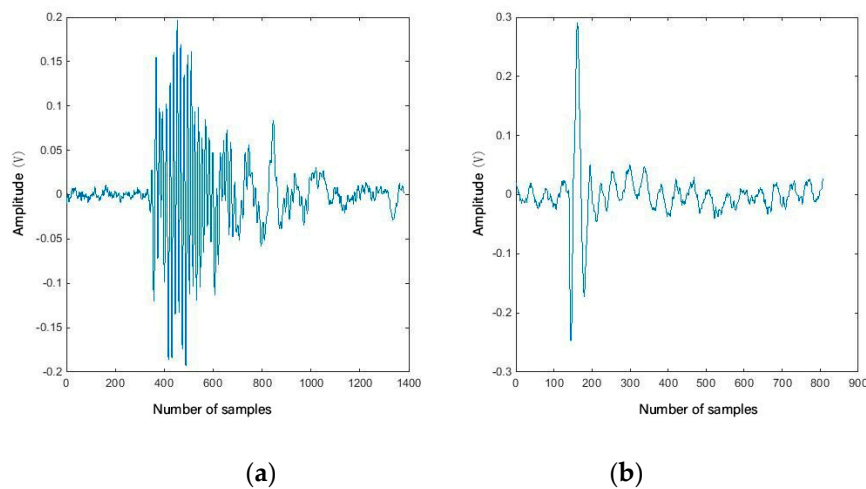
Figure 9. Examples of the two types of signals recorded during the tracing phase: Signals generated by damaged wood (**a**), parasitic electronic and magnetic feedback signals (**b**).

Two types of signals were available: Signals generated by damaged wood and the parasitic electronic and magnetic feedback signals. Figure 8 shows these two signal types.

As shown in Figure 8, the fluctuation of the annual RH of the exhibition hall is roughly the same range (within the red line). Moreover, it can be seen in Figure 6 that the RH fluctuation frequency from June to September is significantly higher than on other months. As a result, RH was pretreated as the daily fluctuation of RH (DFRH) before being compared with the AE parameters (Figure 10). The value of DFRH is obtained by subtracting the lowest relative humidity (RH_{min}) from the highest relative humidity (RH_{max}) of the exhibition hall within 24 h, as shown in Equation (1).

$$DFRH = RH_{max} - RH_{min}, \tag{1}$$
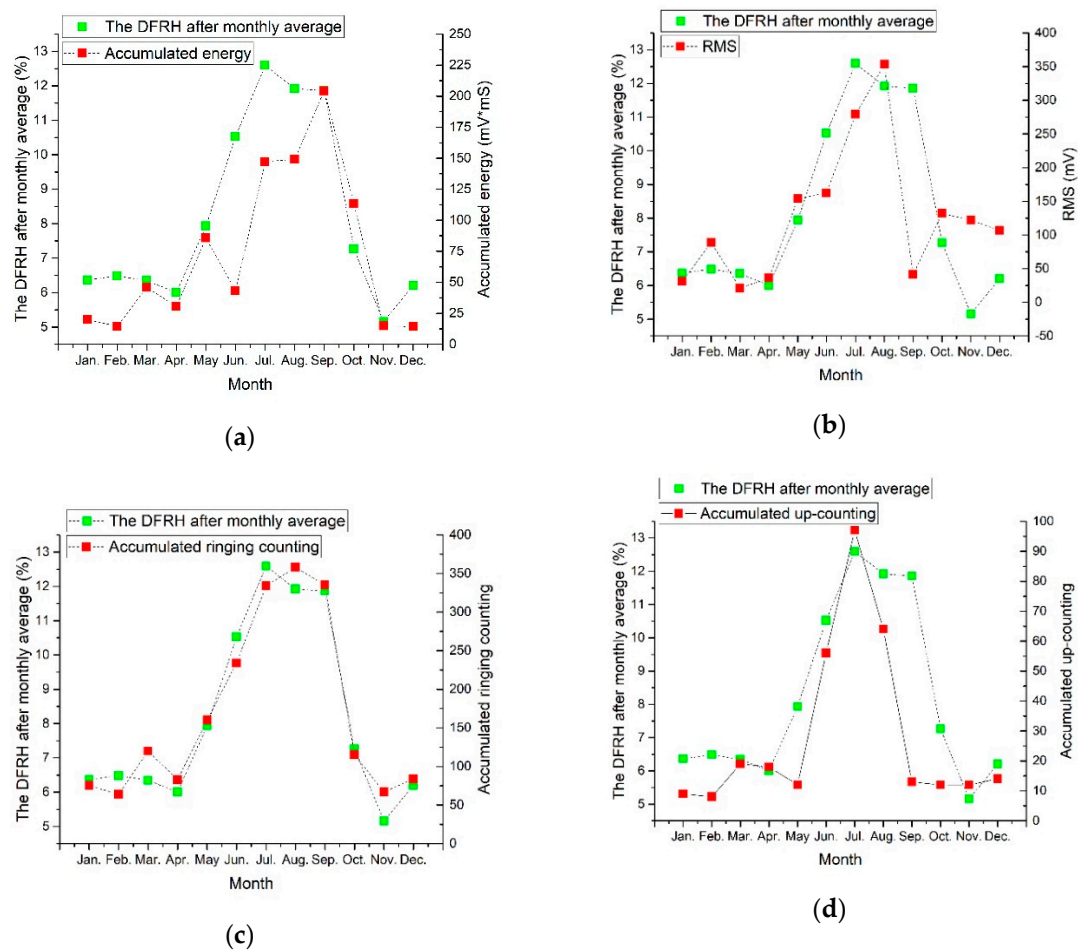
Figure 10. The relationship between acoustic emission parameters and daily fluctuation of relative humidity (DFRH) after monthly average.

Based on Figure 8, accumulated energy (Figure 10a), RMS value (Root Mean Square Voltage, Figure 10b), and accumulated up-counting (Figure 10d) are significantly correlated with DFRH after monthly average. Further, accumulated ringing counting (Figure 10c) is strongly correlated with DFRH after monthly average. In order to quantify this relationship, correlation coefficients between AE parameters and DFRH after monthly average were calculated, as shown in Table 1.

Table 1. Correlation coefficients between AE parameters and DFRH after monthly average. AE: acoustic emission, DFRH: daily fluctuation of relative humidity.

AE Parameter Name	Correlation Coefficient
Accumulated energy	0.83
RMS value (Root Mean Square Voltage)	0.65
Accumulated ringing counting	0.98
Accumulated up-counting	0.77

For Table 1, with increasing DFRH, accumulated ringing counting is increasing. Moreover, as one of the important AE parameters, accumulated ringing counting can reflect the intensity and frequency of damage signals, thereby, being used in the evaluation of AE activity widely. Taken together, the ringing counting can be used as the characteristic parameter to trace the evolution of damage caused by climate-induced stress in wooden cultural objects.

3.2. Analysis of Acoustic Emission Characteristic Parameters

Next, RH was pretreated as DFRH after weekly average that compared with the accumulated ringing counting (Figure 11).
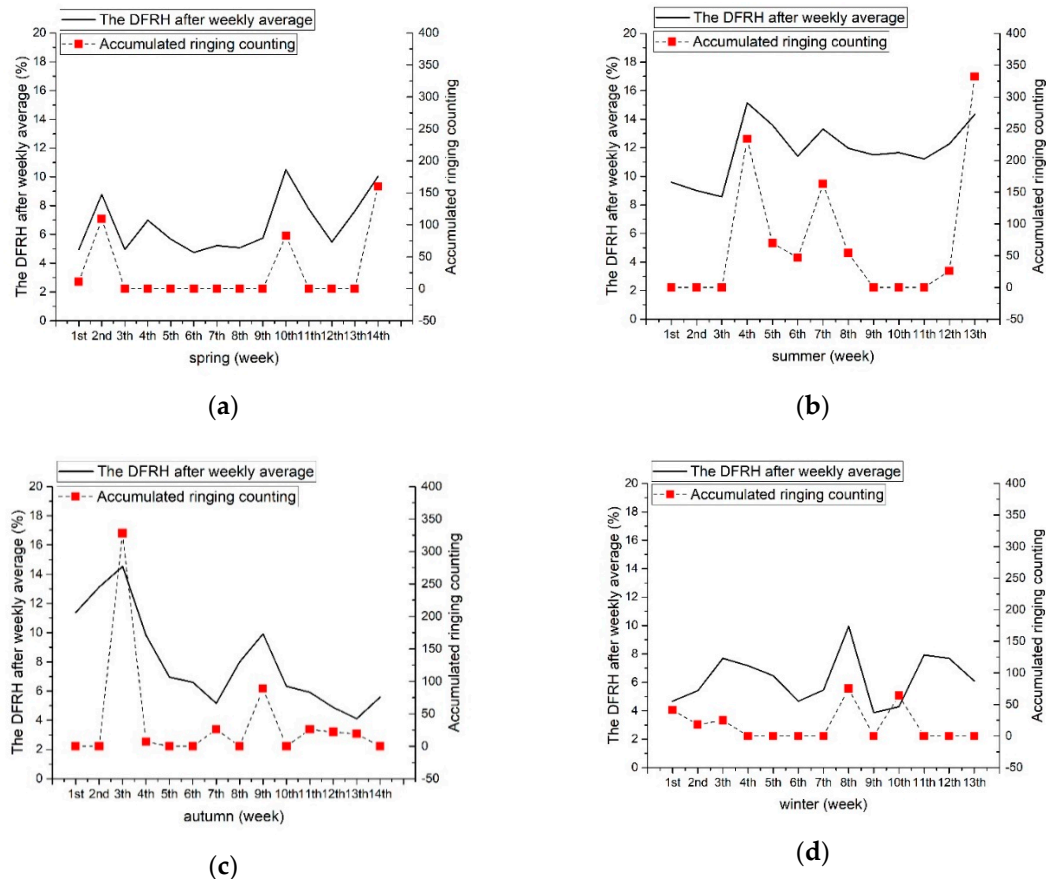
Figure 11. Relationship between DFRH after weekly average and the accumulated ringing counting in spring, summer, autumn, and winter.

As shown in Figure 11, the black broken line represents DFRH after weekly average, and the red squares represent the accumulated ringing counting received by AE sensors. As can be seen in Figure 11, there is a significant positive correlation between DFRH after weekly average and the accumulated ringing counting, that is, the accumulated ringing counting increases with the increase of DFRH. On account of the accumulated ringing counting representing the AE activity, the physical meaning shown in Figure 11 is that the larger DFRH is, the more active the AE activity is, and the more frequent and severe the damage to ancient wooden ships.

In order to analyze the relationship between accumulated ringing counting and DFRH more clearly, the four pictures in Figure 11 were combined (Figure 12).
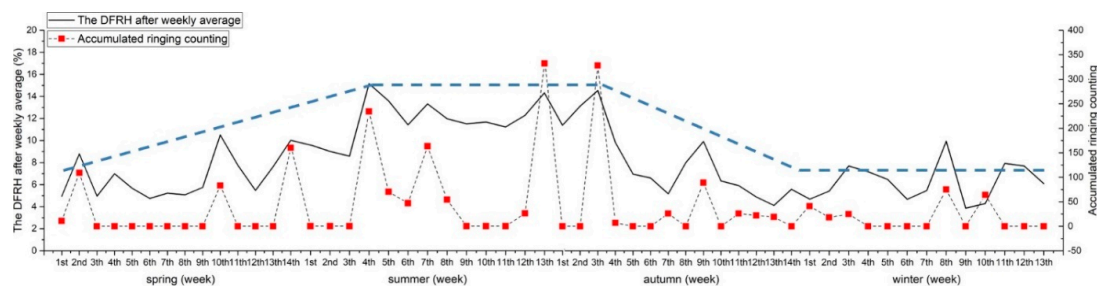
Figure 12. Relationship between DFRH after weekly average and the accumulated ringing counting throughout the year.

Figure 12 shows not only the trend of accumulated ringing counting and DFRH over time, but also the relationship between both. The dotted blue line in the Figure 12 describes the changing trend of DFRH.

Based on Figure 12, it can be seen that both the daily fluctuation and AE activity are increasing with time from March to May. The range of DFRH is the largest since the summer and lasts until September. During this period, the AE activity is also the most intense and concentrated throughout the year, accounting for 60.62% of the annual AE activities. It is not until October that the range of DFRH begins to show a downward trend, and at the same time, the AE activity also decreases. In winter, both the range of DFRH and AE activities are the lowest in the whole year, which is 6.25% per day, 10.72% of the year, respectively.

3.3. Establish the Relationship between DFRH and the Probability of AE Activity

Above all, the ancient wooden ship presents an unstable condition. Thus, moisture content fluctuation should be controlled in this period.

Furthermore, DFRH and accumulated ringing counting were subdivided to analyze the relationship between them (Figure 13).
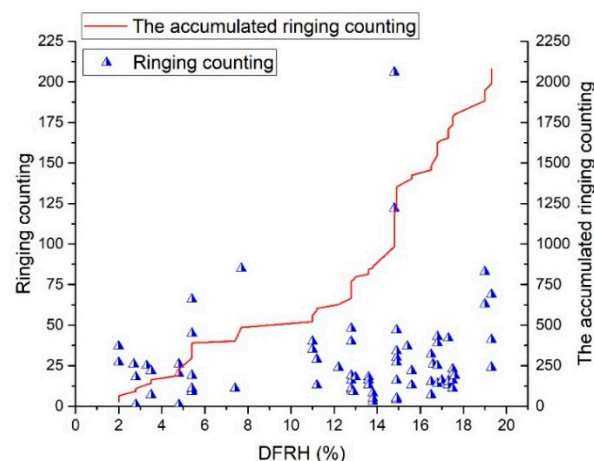
Figure 13. Relationship between DFRH and the accumulated ringing counting, ringing counting.

Figure 13 illustrates the relationship between DFRH and the accumulated ringing counting, ringing counting. In Figure 13, each blue triangle shows an AE event that corresponds to a damage of the ancient wooden ship, and its position in the figure represents DFRH and the ringing counting when the acoustic emission event occurred. Similarly, the red curve represents the accumulated ringing counting. As can be seen in Figure 13, with the increase of DFRH, both AE event and accumulated ringing counting are increasing, that means the damage of the ancient wooden ship is increasing. Combined with Figure 13, further analysis can be given.

The moisture content of wood is an important factor, and it fluctuates with RH. For wooden cultural objects, the moisture content is more susceptible to RH. As the DFRH increases (indicating in the fluctuation of RH), the degree of shrinkage and swelling of the wooden ship increases. This means that the wooden structures are in an unstable state, and the probability of AE activity increases. As shown in Figure 14, with increasing DFRH range, the probability of AE activity increases and approximately presents exponential growth. According to the relationship between DFRH and the probability of AE activity, there is a clear exponential relationship. The relationship between the probability of AE activity and DFRH is obtained by fitting:

$$y = 5.75e^{0.15x}, \tag{2}$$
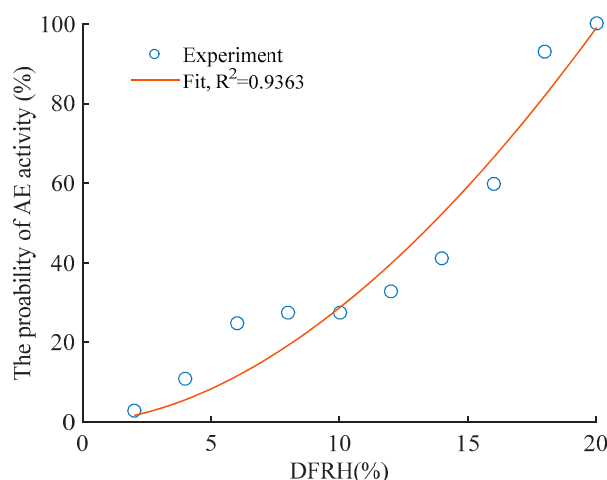
Figure 14. The probability of AE activity of the ancient wooden ship under a different range of DFRH.

We successfully established the relationship between the probability of AE activity and DFRH by means of fitting (the correlation coefficient is 0.93). According to Equation (2), the probability of AE activity is 25% when DFRH equals 10%, and the probability of AE activity is 35% when DFRH equals 12%. It can be concluded from the data that the probability of AE activity increases rapidly when DFRH exceeds 10%. This means that the probability of wood damage increases rapidly, which is not conducive to the long-term preservation of the Song Dynasty shipwreck. Therefore, DFRH cannot exceed 10%. Similarly, the lower the DFRH, the better the preservation of the shipwreck. If the DFRH is too low, it will increase the protection cost of the shipwreck. Therefore, DRFH is equal to 4% (the probability of AE activity is 10%) and is selected as the reference value in this paper. Thus, combined with the physical meaning of AE parameters, the damage rate of ancient wood increase means that the long-term preservation of ancient wooden ship is threatened. From the perspective of the probability of AE activity, this paper proposes to take RH control measures and preferably control DFRH within 4% and no more than 10%.

3.4. Analysis of AE Event Caused by Swelling and Shrinkage

DFRH has two kinds of situations, one is shrinkage, and the other is swelling. Due to the phenomenon of wood shrinkage and swelling, both of them have a certain probability to damage the wood. Therefore, this paper studies the damage conditions of ancient wood caused by two different states (Figure 15).
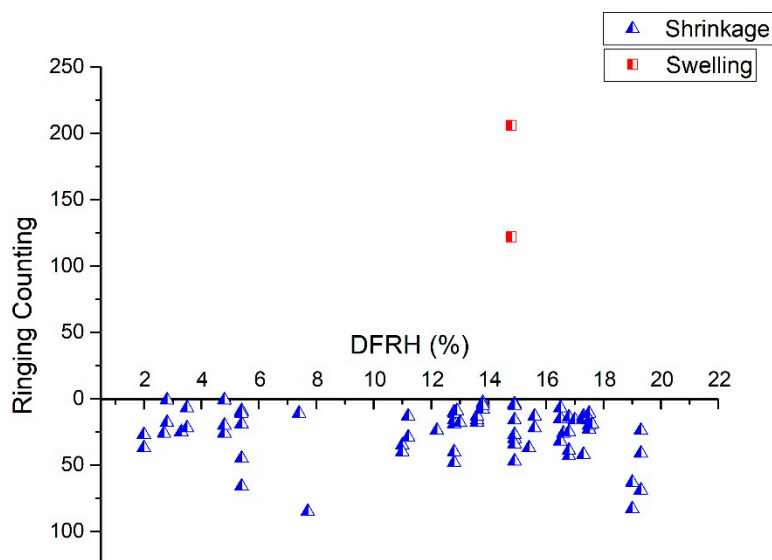
Figure 15. AE activity of ancient wood under the condition of shrinkage and swelling.

Each red square in Figure 15 represents an AE event caused by swelling, and its coordinate showing the position in which DFRH and ringing counting in the AE event occurred. Similarly, each blue triangle represents an AE event caused by shrinkage, and its coordinate showing it's the position in which DFRH and ringing counting in the AE event occurred. It can be seen from Figure 15 that the AE activity of ancient wood during shrinkage is significantly higher than swelling, and AE activity of ancient wood has 84% of the total AE activity (occupy absolute proportion). As shown by the blue dotted line in Figure 15, at the same time, the minimum diurnal variation in RH causing AE event under shrinkage status is 2.0%, while the data under swelling reaches up to 14.8% (red dotted line in Figure 15).

4. Conclusions

The tracing of acoustic emission proved an effective non-destructive method of indicating the damage in wooden cultural objects exposed to variations in RH at historic sites or during their transportation. The accumulated ringing counting is positively correlated with DFRH that are known to be one of the main factors that contribute to the deterioration of wooden objects, so it can be used for tracing the damage of ancient wooden cultural heritage. The range of DFRH directly affects the health status of ancient wood: The wider it is, the higher the probability of damage, and the more harm to the long-term preservation of ancient ships. The relationship between the probability of AE activity and the daily DFRH is established. DFRH is equal to 10%, which can be used as a critical condition for judging whether the health condition of ancient wooden ships is threatened. Compared with the state of swelling, the damage of ancient wooden ships is more likely to occur in the state of shrinkage. It is recommended that the scope of DFRH should be controlled within 4%, and if 10% is exceeded, an alarm would be activated, warning the staff of the increased risk of mechanical damage to an ancient wooden ship. This provides evidence for the development of special equipment for wood monitoring.

5. Patents

In this paper, a kind of sound insulation cabin was designed and a patent was applied (CN207231626U).

Author Contributions: D.Z. and J.Z. conceived this study, and Q.Z. and L.F. established the AE monitoring system and conducted the experiments. L.F. provided test site and subjects. Q.Z. and J.Z. implemented and analyzed the experimental results. Q.Z. and D.Z. wrote the manuscript.

Funding: This research was funded by Beijing Natural Science Foundation, grant number 2182045.

Acknowledgments: We are grateful to Jianzhong Zhang from Beijing Forestry University, Beijing, China, for his help during the laboratory analysis research.

Conflicts of Interest: The authors declare no conflict of interest.

References

1. Fei, L.H. An investigation of the state of conservation of the Song Dynasty Shipwreck in Quanzhou Bay. *China Cult. Herit. Sci. Res.* **2014**, *2*, 74–79. [CrossRef]

2. Fei, L.H.; Li, G.Q. Forty years of conservation: A Song Dynasty shipwreck from the Quanzhou Bay. *Sci. Conserv. Archaeol.* **2015**, *27*, 95–100. [CrossRef]

3. Salinas, C.; Chavez, C.; Ananias, R.A.; Elustondo, D. Unidimensional Simulation of Drying Stress in Radiata Pine Wood. *Dry. Technol.* **2015**, *33*, 996–1005. [CrossRef]

4. Mizuno, S.; Torizu, R.; Sugiyama, J. Wood identification of a wooden musk using synchrotron X-ray microtomography. *J. Archaeol. Sci.* **2010**, *37*, 2842–2845. [CrossRef]

5. Stelzner, J.; Million, S. X-ray Computed Tomography for the anatomical and dendrochronological analysis of archaeological wood. *J. Archaeol. Sci.* **2015**, *55*, 188–196. [CrossRef]

6. Tomasini, E.P.; Gomez, B.; Halac, E.B.; Reinoso, M.; Liscia, J.D.; Siracusano, G.; Maier, M.S. Identification of carbon-based black pigments in four south American polychrome wooden sculptures by Raman microscopy. *Herit. Sci.* **2015**, *3*, 19. [CrossRef]

7. Park, J.; Schilling, M.R.; Khanjian, H.; Lee, J.Y. Stratigraphic Examination of a Korean Lacquered Wooden Coffin Sample by Pyrolysisi/GC/MS. *Chromatographia* **2018**, *81*, 1685–1694. [CrossRef]

8. Howe, E.; Kapla, E.; Newman, R.; Frantz, J.H.; Pearlstein, E.; Levinson, J. The occurrence of a titanium dioxide/silica white pigment on wooden Andean qeros: A cultural and chronological marker. *Herit. Sci.* **2018**, *6*, 41. [CrossRef]

9. Colombini, M.P.; Lucejko, J.J.; Modugno, F.; Orlandi, M.; Tolppa, E.L.; Zoia, L. A multi-analytical study of degradation of lignin in archaeological waterlogged wood. *Talanta* **2009**, *80*, 61–70. [CrossRef] [PubMed]

10. Sandak, A.; Sandak, J.; Zborowska, M.; Pradzynski, W. Near infrared spectroscopy as a tool for archaeological wood characterization. *J. Archaeol. Sci.* **2010**, *37*, 2093–2101. [CrossRef]

11. Lobb, M.; Krawiec, K.; Howard, A.J.; Gearey, B.R.; Chapman, H.P. A new approach to recoring and monitoring wet-preserved archaeological wood using three-dimensional laser scanning. *J. Archaeol. Sci.* **2010**, *37*, 2995–2999. [CrossRef]

12. Nowak, T.P.; Jasienko, J.; Bielecka, K.H. In situ assessment of structural timber using the resistance drilling method- Evaluation of usefulness. *Constr. Build. Mater.* **2016**, *102*, 403–415. [CrossRef]

13. Tamburini, D.; Lucejko, J.J.; Zborowska, M.; Modugno, F.; Pradzynski, W.; Colombini, M.P. Archaeological wood degradation at the site of Biskupin (Ploand): Wet chemical analysis and evaluation of specific Py-GC/MS profiles. *J. Anal. Appl. Pyrolysis* **2015**, *115*, 7–15. [CrossRef]

14. Tamburini, D.; Lucejko, J.J.; Modugno, F.; Colombini, M.P. Combined pyrolysis-based techniques to evaluate the state of preservation of archaeological wood in the presence of consolidating agents. *J. Anal. Appl. Pyrolysis* **2016**, *122*, 429–441. [CrossRef]

15. Tamburini, D.; Lucejko, J.J.; Pizzo, B.; Mohammed, M.Y.; Sloggett, R.; Colombini, M.P. A critical evaluation of the degradation state of dry archaeological wood from Egypt by SEM, ATR-FTIR, wet chemical analysis and Py(HMDS)-GC-MS. *Ploym. Degrad. Stab.* **2017**, *146*, 140–154. [CrossRef]

16. Raposo, P.C.; Andrade, M.; Correia, J.A.F.O.; Salavessa, M.E.; Reis, C.; Oliveira, C.; Jesus, A.D. Non-Destructive Structural Wood Diagnosis of a Medieval Building. In Proceedings of the 2nd International Conference on Structural Integrity, Funchal, Madeira, Portugal, 4–7 September 2017; Volume 5, pp. 1141–1152. [CrossRef]

17. Bardet, M.; Gerbaud, G.; Tran, Q.H.; Hediger, S. Study of interactions between polyethylene glycol and archaeological wood components by 13C high-resolution solid-state CP-MAS NMR. *J. Archaeol. Sci.* **2007**, *34*, 1670–1676. [CrossRef]

18. Poli, T.; Chiantore, O.; Nervo, M.; Piccirillo, A. Mid-IR fiber-optic reflectance spectroscopy for identifying the finish on wooden furniture. *Anal. Bioanal. Chem.* **2011**, *400*, 1161–1171. [CrossRef]

19. Henriques, D.F.; Neves, A.S. Semi-destructive in situ tests as support to the assessment of a conservation process. *Constr. Build. Mater.* **2015**, *101*, 1253–1258. [CrossRef]

20. Sfarra, S.; Castanedo, C.I.; Ridolfi, S.; Cerichelli, G.; Ambrosini, D.; Paoletti, D.; Maldague, X. Holographic Interferometry (HI), Infrared Vision and X-ray Fluorescence (XRF) spectroscopy for the assessment of painted wooden statues: A new integrated approach. *Appl. Phys. A* **2014**, *115*, 1041–1056. [CrossRef]

21. Re, A.; Albertin, F.; Avataneo, C.; Brancaccio, R.; Corsi, J.; Cotto, G.; Blasi, S.D.; Dughera, G.; Durisi, E.; Ferrarese, W.; et al. X-ray tomography of large wooden artworks: the case study of "Doppio corpo" by Pietro Piffetti. *Herit. Sci.* **2014**, *2*, 19. [CrossRef]

22. Bulcke, J.V.D.; Denis, V.L.; Dierick, M.; Masschaele, B.; Hoorebeke, L.V.; Acker, J.V. Nondestructive research on wooden musical instruments: From macro-to microscale imaging with lab-based X-ray CT systems. *J. Cult. Herit.* **2017**, *27*, 78–87. [CrossRef]

23. Perez, M.A.; Manjon, A.; Ray, J.; Lopez, R.S. Experimental assessment of the effect of an eventual non-invasive intervention on a Torres guitar through vibration testing. *J. Cult. Herit.* **2017**, *27*, 103–111. [CrossRef]

24. Fang, Y.M.; Lin, L.J.; Feng, H.L.; Lu, Z.X.; Emms, G.W. Review of the use of air-coupled ultrasonic technologies for nondestructive testing of wood and wood products. *Comput. Electron. Agric.* **2017**, *137*, 79–87. [CrossRef]

25. Senni, L.; Casieri, C.; Bovino, A.; Gaetani, M.C.; Luca, F.D. A portable NMR sensor for moisture monitoring of wooden works of art, particularly of paintings on wood. *Wood Sci. Technol.* **2009**, *43*, 167–180. [CrossRef]

26. Konopka, D.; Ehricht, S.; Kaliske, M. Hygro-mechanical investigations of clavichord replica at cyclic climate load: Experiments and simulations. *J. Cult. Herit.* **2019**, *36*, 210–221. [CrossRef]

27. Ristschel, F.; Brunner, A.J.; Niemz, P. Nondestructive evaluation of damage accumulation in tensile test specimens made from solid wood and layered wood materials. *Compos. Struct.* **2013**, *95*, 44–52. [CrossRef]

28. Bucur, V. *Acoustics of Wood*; Springer: Berlin/Heidelberg, Germany, 2006.

29. Ansell, M.P. Acoustic emission from softwoods in tension. *Wood Sci. Technol.* **1982**, *16*, 35–57. [CrossRef]

30. Rescalvo, F.J.; Aguilar-Aguilera, A.; Suarez, E.; Valverde-Palacios, I.; Gallego, A. Acoustic emission during wood-CFRP adhesion tests. *Int. J. Adhes. Adhes.* **2018**, *87*, 79–90. [CrossRef]

31. Perrin, M.; Yahyaoui, I.; Gong, X.J. Acoustic monitoring of timber structures: Influence of wood species under bending loading. *Constr. Build. Mater.* **2019**, *208*, 125–134. [CrossRef]

32. Vautrin, A.; Harris, B. Acoustic emission characterization of flexural loading damage in wood. *J. Mater. Sci.* **1987**, *22*, 3707–3716. [CrossRef]

33. Reiterer, A.; Stanzl-Tschegg, S.E.; Tschegg, E.K. Mode I fracture and acoustic emission of softwood and hardwood. *Wood Sci. Technol.* **2000**, *34*, 417–430. [CrossRef]

34. Rice, R.W.; Skaar, C. Acoustic emission patterns from the surfaces of red oak wafers under transverse bending stress. *Wood Sci. Technol.* **1990**, *24*, 123–129. [CrossRef]

35. Lee, S.H.; Quarles, S.L.; Schniewind, A.P. Wood fracture, acoustic emission, and the drying process. Part 2. Acoustic emission pattern recognition analysis. *Wood Sci. Technol.* **1996**, *38*, 283–292. [CrossRef]

36. Nowakowska, M.; Krajewski, A.; Witomski, P.; Bobinski, P. Thermic limitation of AE detection method of old house borer larvae (*Hyloturpes bajulus L.*) in wooden structures. *Constr. Build. Mater.* **2017**, *136*, 446–449. [CrossRef]

37. Kowalski, S.J.; Musielak, W.G. The identification of fracture in dried wood based on theoretical modelling and acoustic emission. *Wood Sci. Technol.* **2004**, *38*, 35–52. [CrossRef]

38. Lamy, F.; Takarli, M.; Angellier, N.; Dubois, F.; Pop, O. Acoustic emission technique for fracture analysis in wood materials. *Int. J. Fract.* **2015**, *192*, 57–70. [CrossRef]

39. Schniewing, A.P.; Quarles, S.L.; Lee, S.H. Wood fracture, acoustic emission, and the drying process: Part 1. Acoustic emission associated with fracture. *Wood Sci. Technol.* **1996**, *30*, 273–281. [CrossRef]

40. Rescalvo, F.J.; Suarez, E.; Palacios, I.V.; Santiago-Zaragoza, J.M.; Gallego, A. Health monitoring of timber beams retrofitted with carbon fiber composites via the acoustic emission technique. *Compos. Struct.* **2018**, *206*, 392–402. [CrossRef]

41. Diakhate, M.; Bastidas-Arteaga, E.; Pitti, R.M.; Schoefs, F. Cluster analysis of acoustic emission activity within wood material: Towards a real-time monitoring of crack tip propagation. *Eng. Fract. Mech.* **2017**, *180*, 254–267. [CrossRef]

42. Ando, K.; Hirashima, Y.; Sugihara, M. Microscopic processes of shearing fracture of old wood, examined using the acoustic emission technique. *J. Wood Sci.* **2006**, *52*, 483–489. [CrossRef]

43. Jakiela, S.; Bratasz, L.; Kozlowski, R. Acoustic emission for tracing the evolution of damage in wooden objects. *Stud. Conserv.* **2007**, *52*, 101–109. [CrossRef]

44. Jakiela, S.; Bratasz, L.; Kozlowski, R. Acoustic emission for tracing fracture intensity in lime wood due to climatic variation. *Wood Sci. Technol.* **2008**, *42*, 269–279. [CrossRef]

45. Conte, S.L.; Vaiedelich, S.; Thomas, J.H.; Muliava, V.; Reyer, D.D.; Maurin, E. Acoustic emission to detect xylophagous insects in wooden musical instrument. *J. Cult. Herit.* **2015**, *16*, 338–343. [CrossRef]